Supporting Information

for

Molecular Dynamic Simulation of Prenucleation of Apatite at a Type-I Collagen Template: Ion Association and Mineralization Control

Zhiyu Xue[1], Xin Wang[1] and Dingguo Xu*[1,2]

[1]MOE Key Laboratory of Green Chemistry and Technology, College of Chemistry, Sichuan University, Chengdu, Sichuan, 610064 PR China

[2] Research Center for Materials Genome Engineering, Sichuan University, Chengdu, Sichuan, 610065, PR China

* To whom correspondence should be addressed: dgxu@scu.edu.cn (D.X), Tel: 86-28-85406156.

Contents

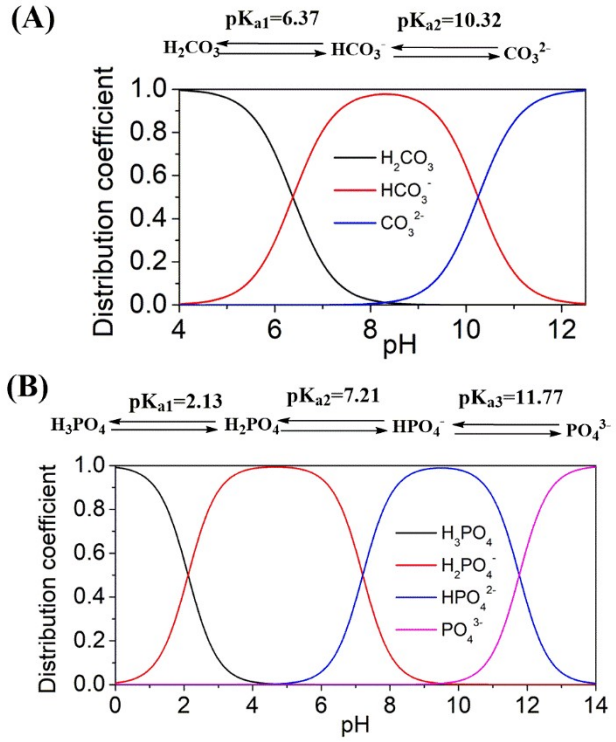

Figure S1. (A) The pH distribution coefficient of carbonate. (B) The pH distribution coefficient of phosphate.

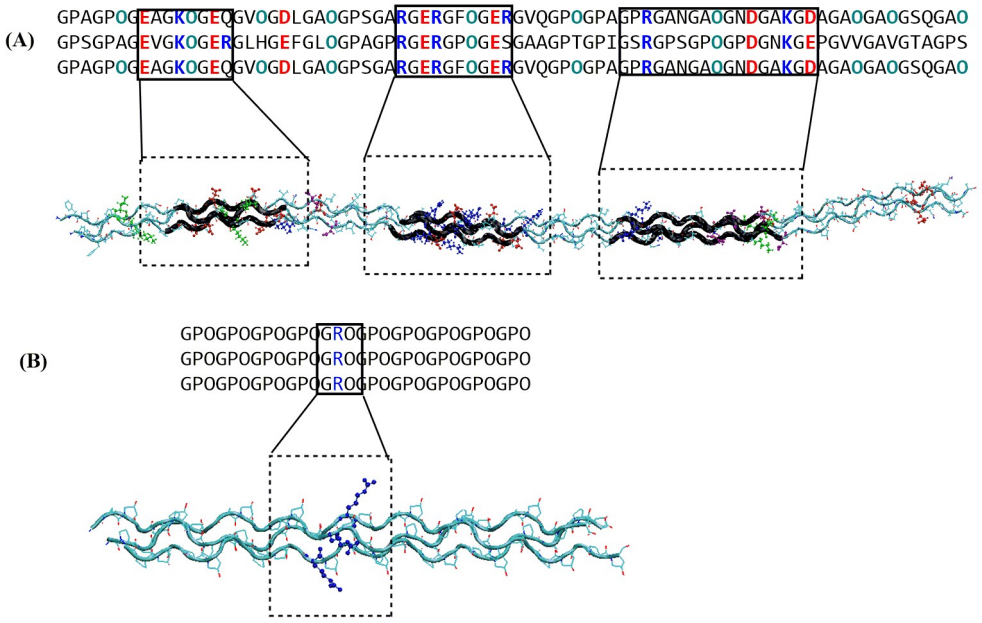

Figure S2. Amino acid sequence of the type-I collagen protein and CMP model. (A) for type-I and (B) for CMP.

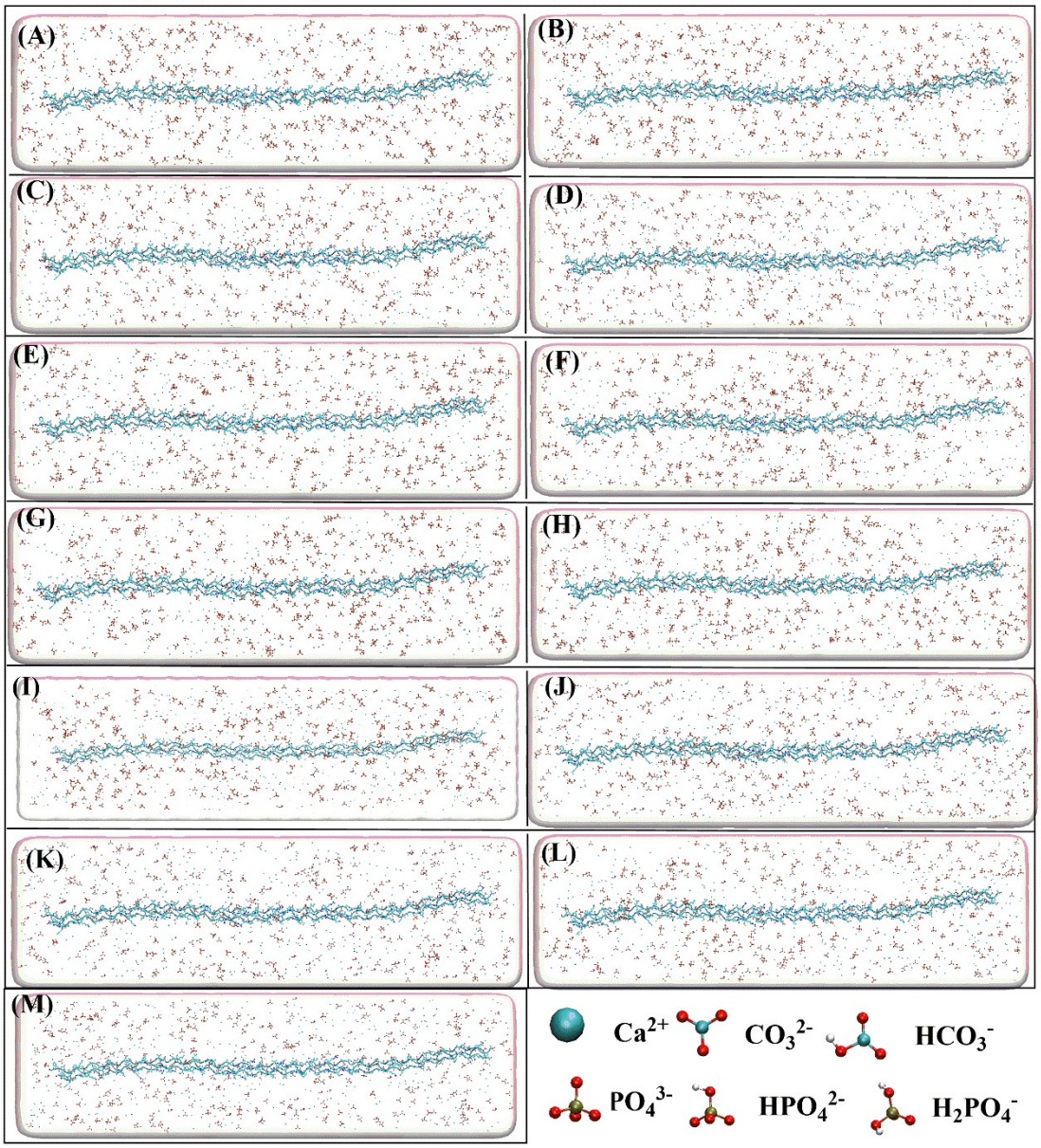

Figure S3. The initial states of collagen models in the aqueous phase. (A) Model 1, (B) Model 2, (C) Model 3, (D) Model 4, (E) Model 5, (F) Model 6**,** (G) Model 7, (H) Model 8, (I) Model 9, (J) Model 10, (K) Model 11, (L) Model 12 and (M) Model 13

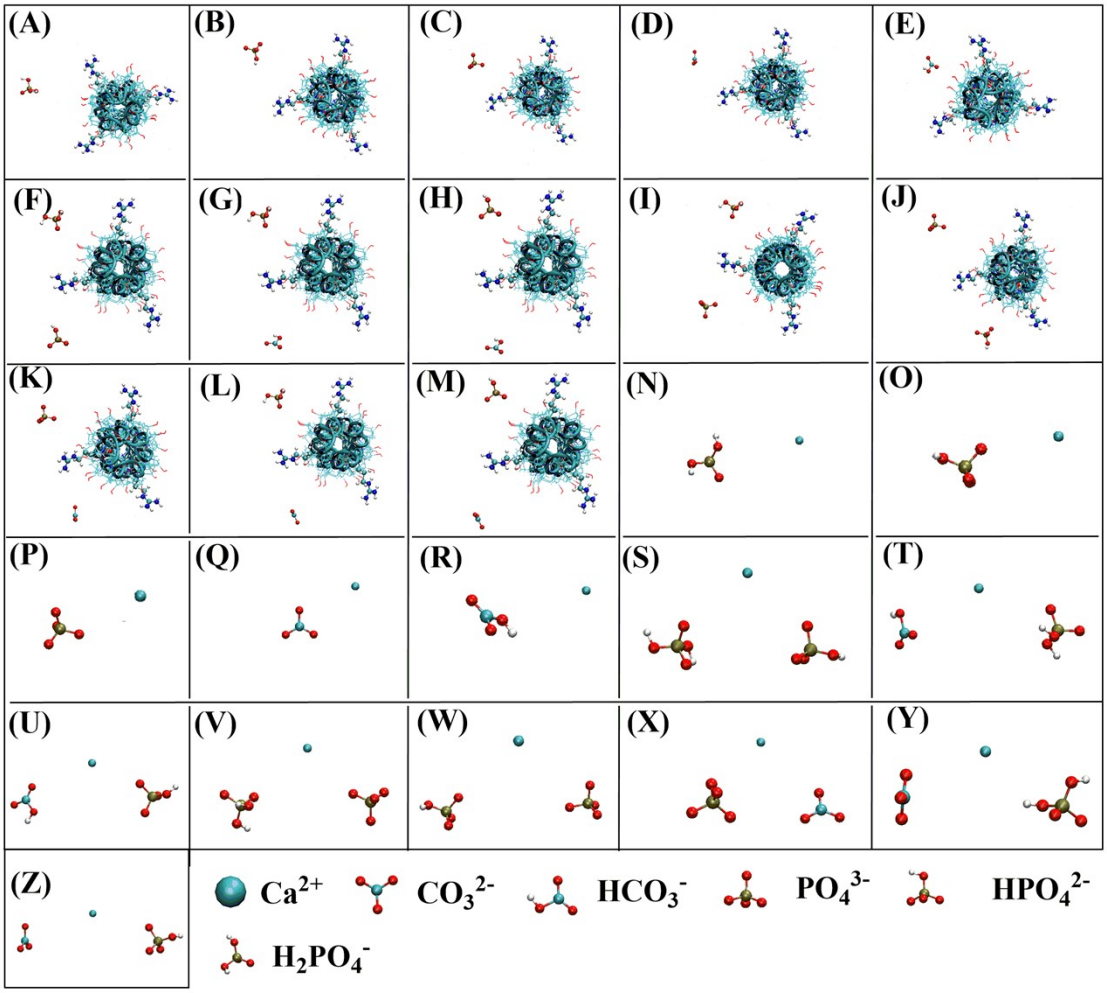

Figure S4. The 26 initial states of collagen models in metdynamics calculations, for which the corresponding definitions are listed in Table S2. (A) System 1, (B) System 2, (C) System 3, (D) System 4, (E) System 5, (F) System 6**,** (G) System 7, (H) System 8, (I) System 9, (J) System 10, (K) System 11, and (L) System 12, (M) System 13, (N) System 14, (O) System 15, (P) System 16, (Q) System 17, (R) System 18, (S) System 19, (T) System 20**,** (U) System 21, (V) System 22, (W) System 23, (X) System 24, (Y) System 25, and (Z) System 26.

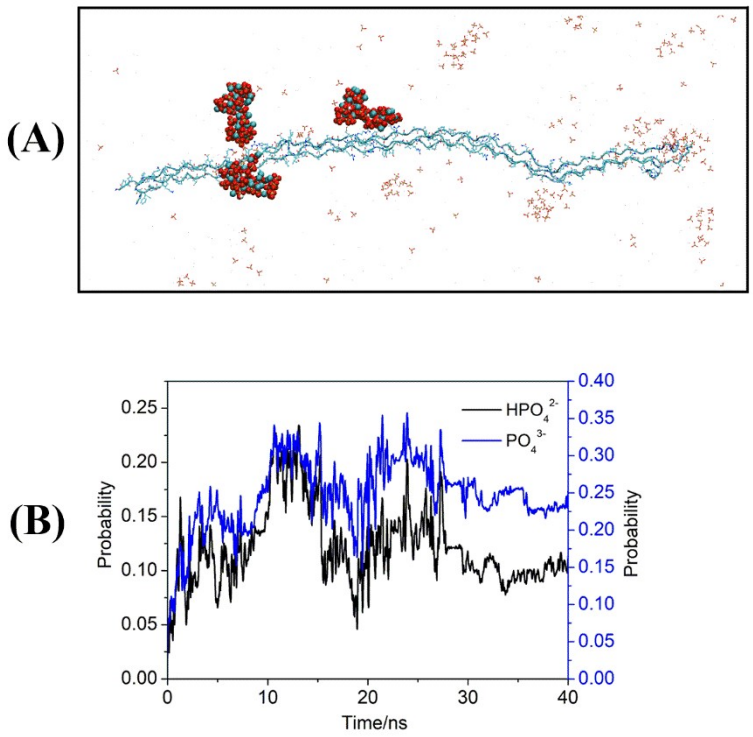

Figure S5. (A) Snapshots of calcium phosphate nucleation promoted by type I collagen in presence of PO_4^{3-} for models containing 0.20 M PO_4^{3-} and 0.04 M HPO_4^{2-} with 40 ns molecular dynamics. (B) Evolution of probability of various ions in 40 ns molecular dynamics simulations of models containing 0.20 M PO_4^{3-} and 0.04 M HPO_4^{2-}.

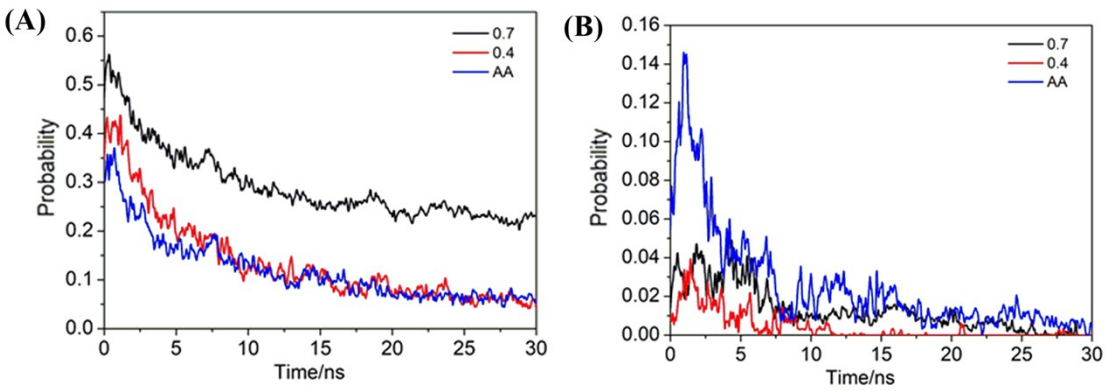

Figure S6. Evolution of probability of HPO_4^{2-} along the 30 ns MD simulation time for models containing 0.4 M and 0.7 M ionic concentration. (A) in the collagen surface. (B) in the solution.

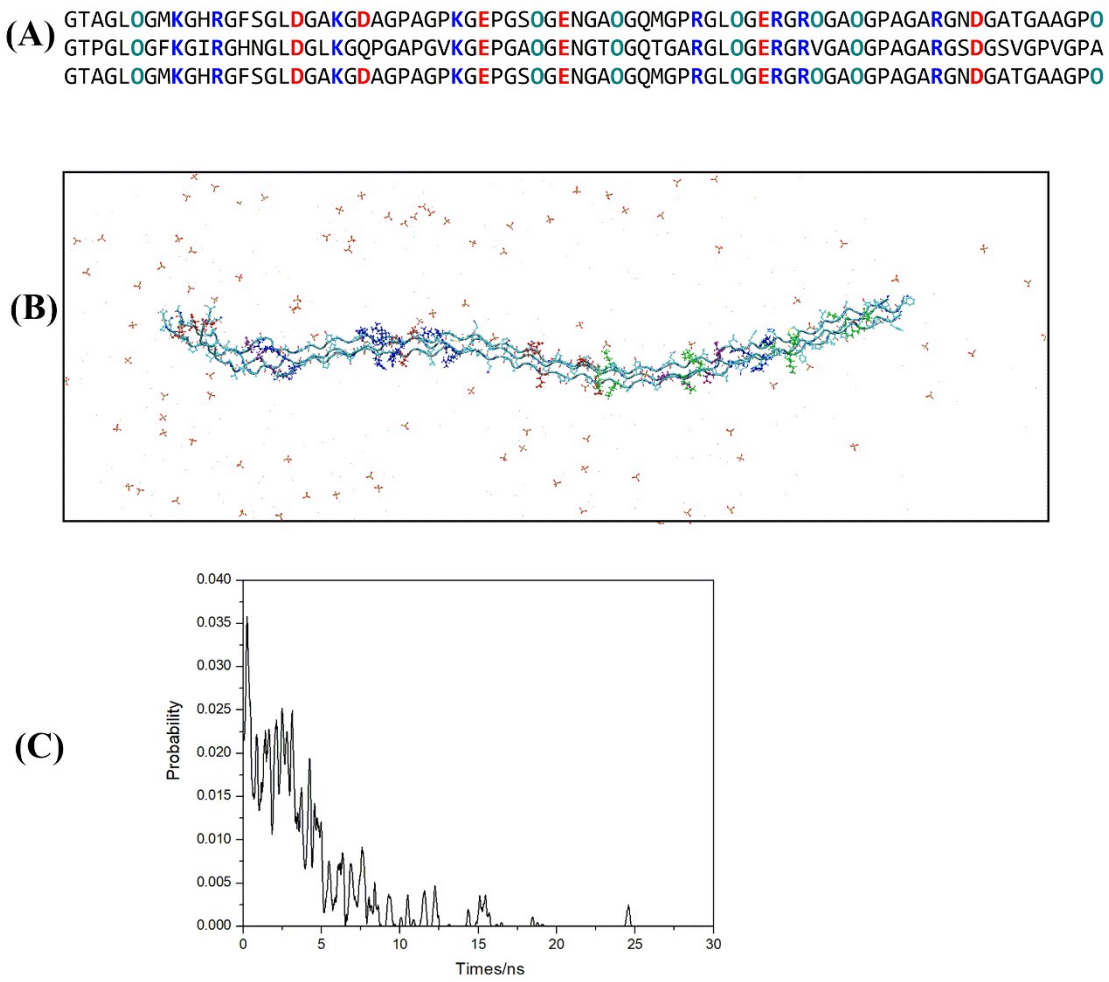

Figure S7. (A) Amino acid sequence of the other type-I collagen protein. (B) Snapshots of calcium phosphate nucleation promoted by type I collagen in presence of PO_4^{3-} for models containing 0.24 M HPO_4^{2-}. (C) Evolution of probability of various ions in 30 ns molecular dynamics simulations of models containing 0.24 M HPO_4^{2-}.

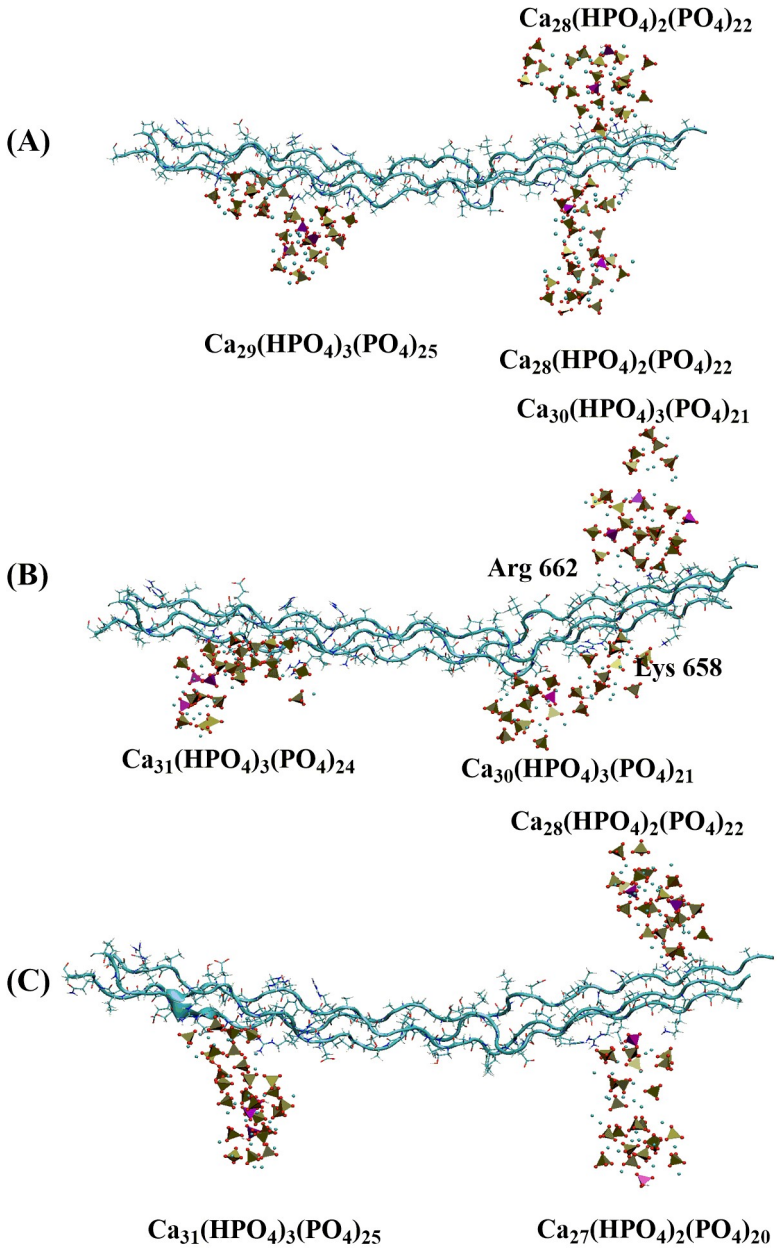

Figure S8. Nucleation sites and cluster morphologies of three replicas which are discussed in the manuscript. (A), (B)and (C) for model 7.

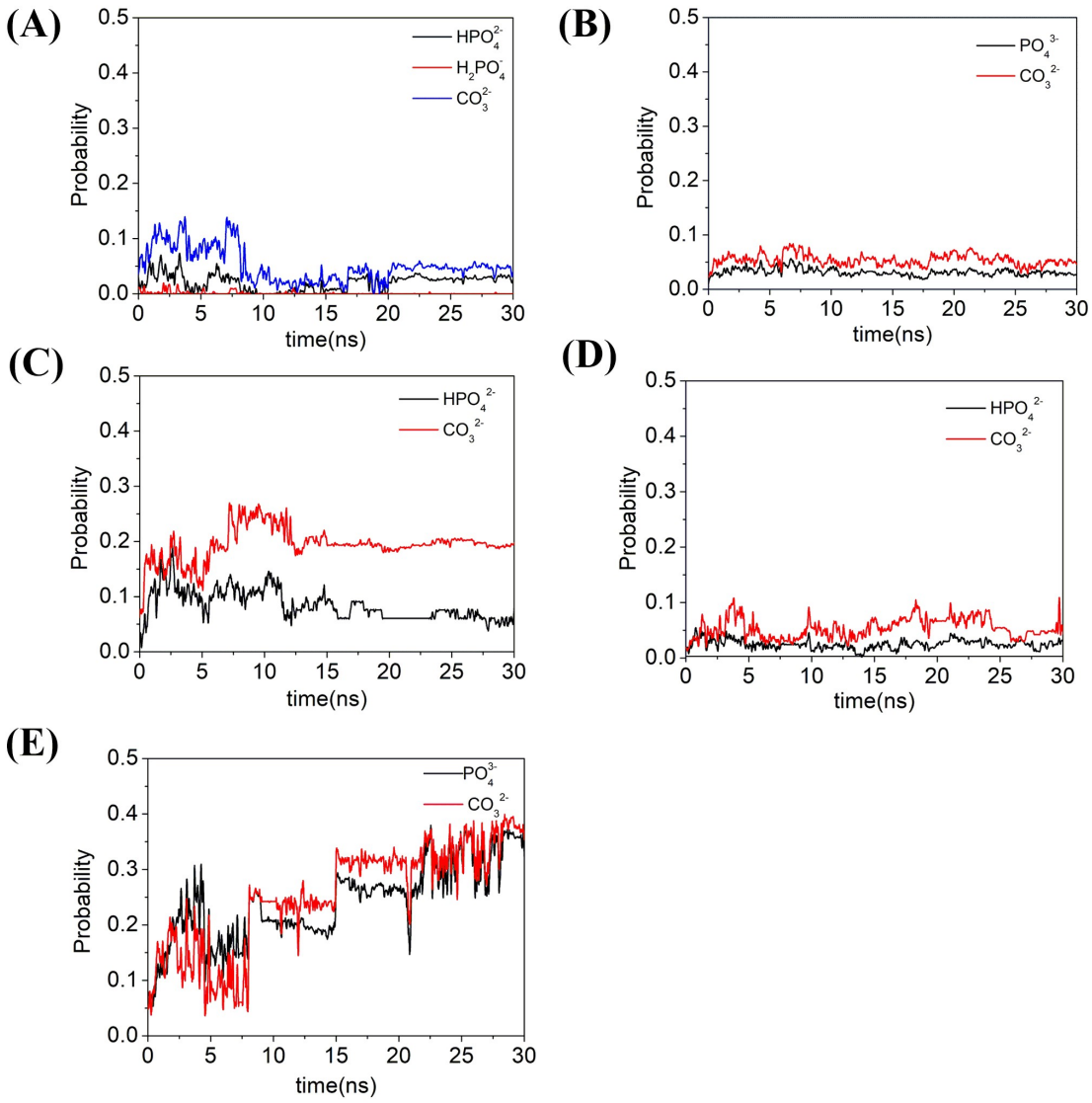

Figure S9. Evolution of the probability of various ions ($H_2PO_4^-$, HPO_4^{2-}, PO_4^{3-}, and CO_3^{2-}) in 30 ns molecular dynamics simulations of models containing (A) Model 9. (B) Model 10. (C) Model 11. (D) Model 12. (E) Model 13.

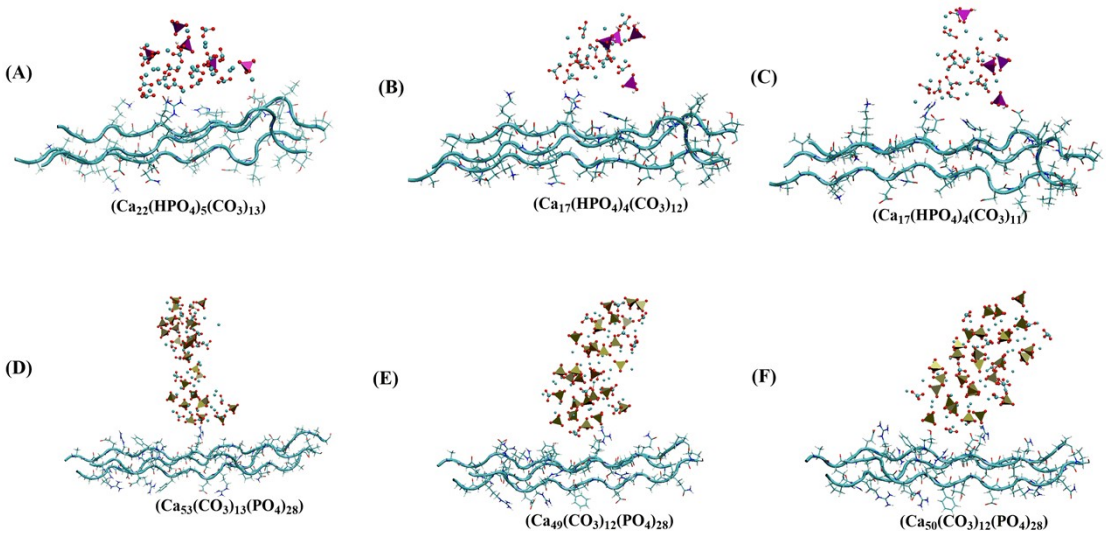

Figure S10. Nucleation sites and cluster morphologies of three replicas which are discussed in the manuscript. (A), (B)and (C) for model 11. (D), (E)and (F) for model 13

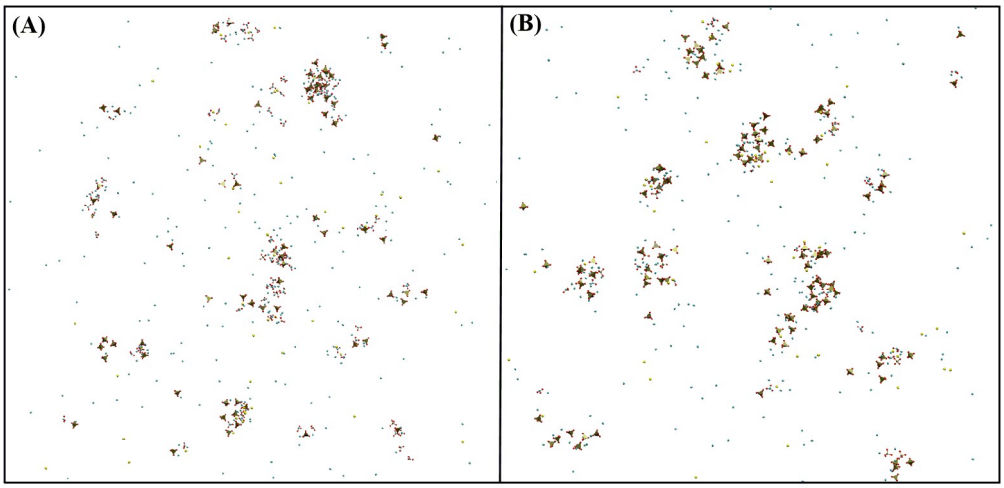

Figure S11. Snapshots for the nucleation of calcium phosphate in the absence of a collagen molecule after 30 ns, for which the system contains only Ca2+, PO43-, and CO32- but with different concentration ratios. (A) PO43-/CO32- = 1:1 and (B) PO43-/CO32- = 5:1.

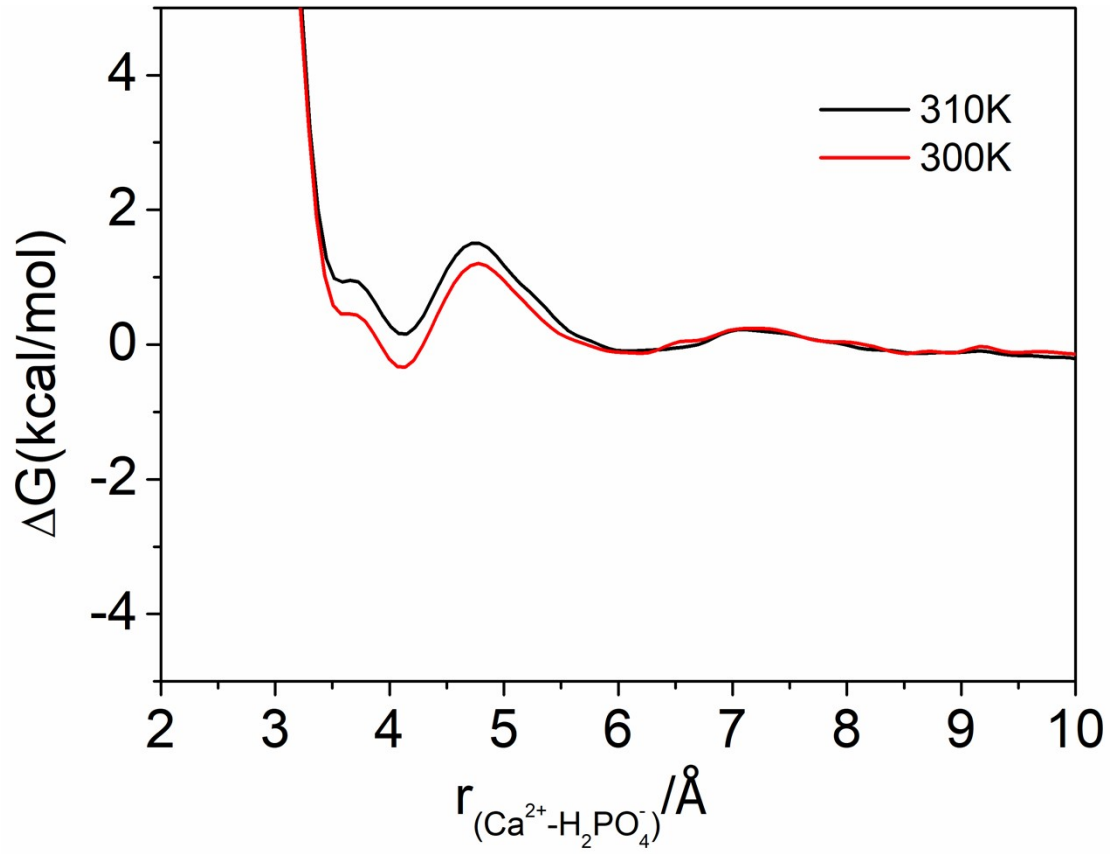

Figure S12. Free energy profiles for the Ca^{2+}-$H_2PO_4^-$ system at the temperature of 300 K and 310 K, respectively.

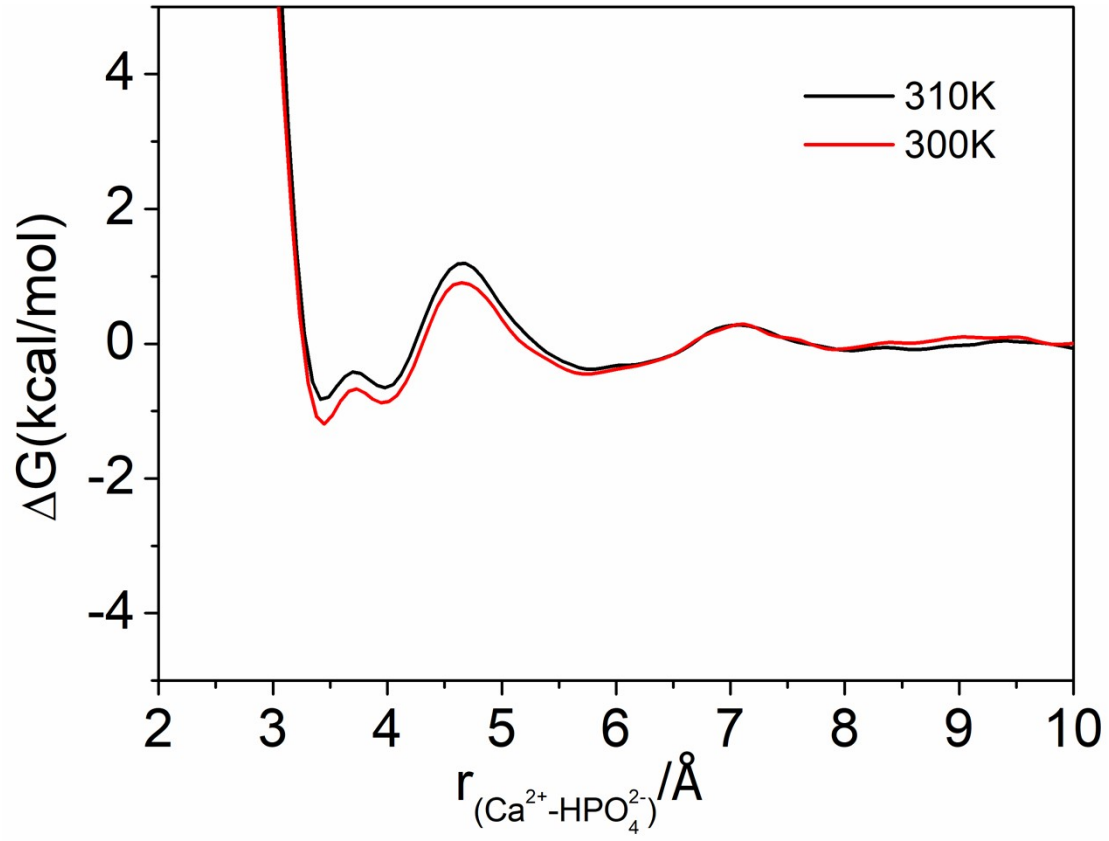

Figure S13. Free energy profiles for the Ca^{2+}-HPO_4^- system at the temperature of 300 K and 310 K, respectively.

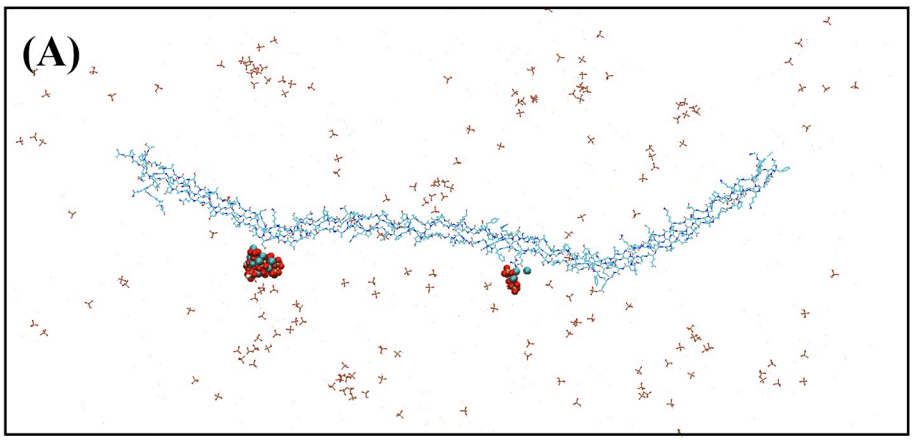

Figure S14. Snapshots of calcium phosphate nucleation promoted by type I collagen in presence of PO_4^{3-} for models containing 0.08 M $H_2PO_4^-$, 0.08 M CO_3^{2-}, and 0.08 M PO_4^{3-}.

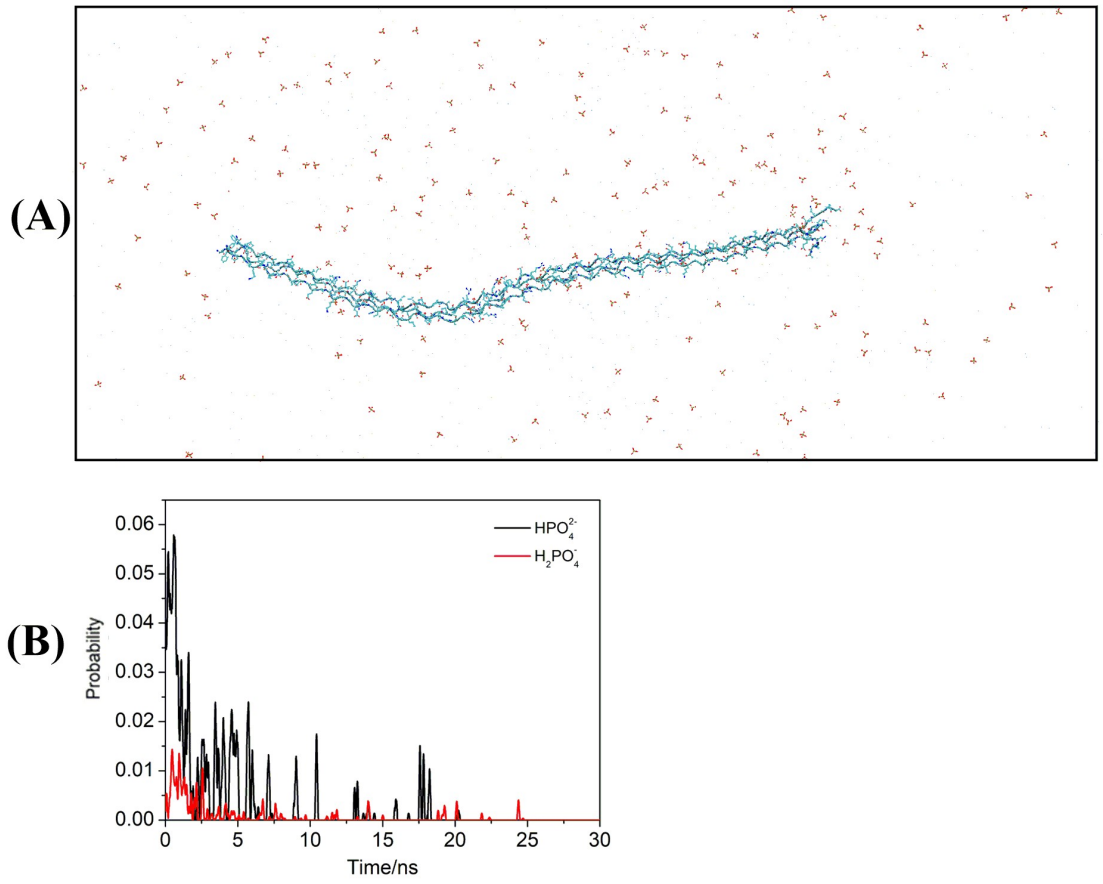

Figure S15. (A) Snapshots of calcium phosphate nucleation promoted by type I collagen in presence of PO_4^{3-} for models containing 0.20 M HPO_4^{2-} and 0.04 M $H_2PO_4^-$. (B) Evolution of the probability of various ions in 30 ns molecular dynamics simulations of models containing 0.20 M HPO_4^{2-} and 0.04 M $H_2PO_4^-$.

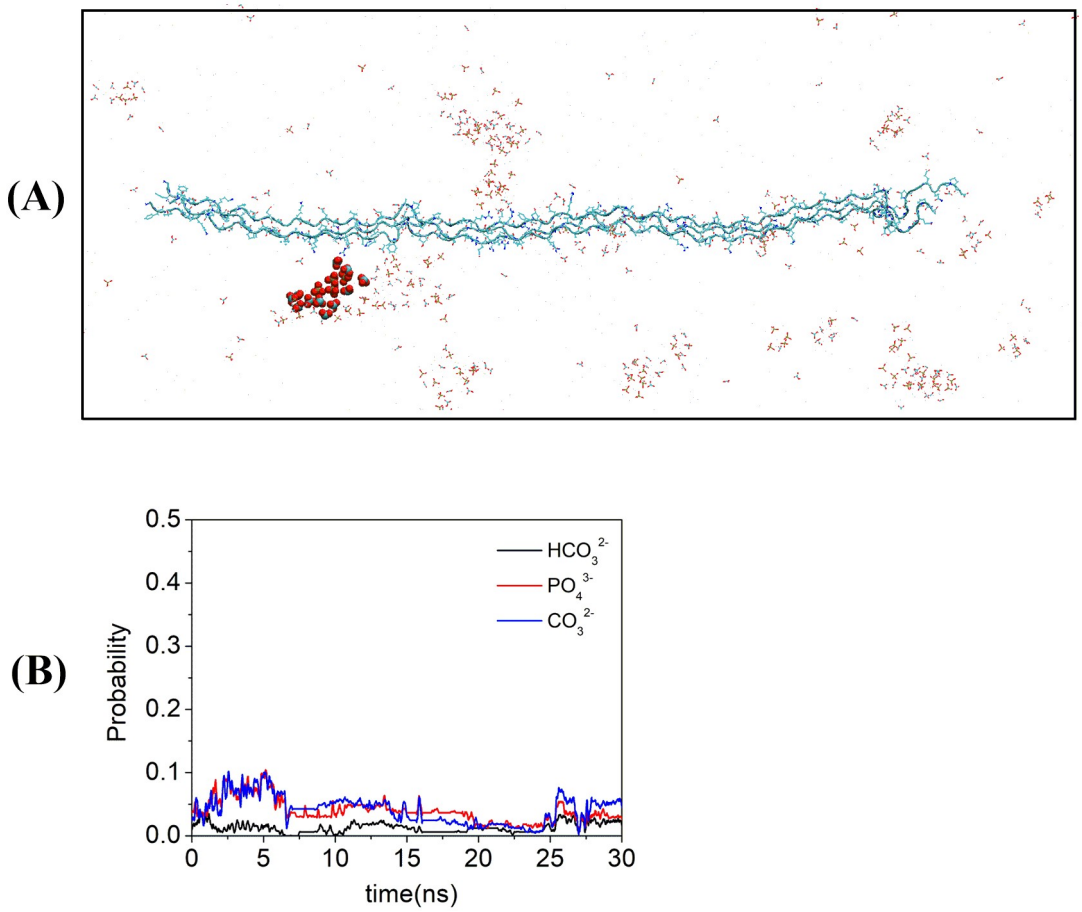

Figure S16. (A) Snapshots of calcium phosphate nucleation promoted by type I collagen in presence of PO_4^{3-} for models containing 0.08 M HCO_3^- , 0.08 M PO_4^{3-}, and 0.08 M CO_3^{2-}. (B) Evolution of probability of various ions in 30 ns molecular dynamics simulations of models containing 0.08 M HCO_3^-, 0.08 M PO_4^{3-}, and 0.08 M CO_3^{2-}.

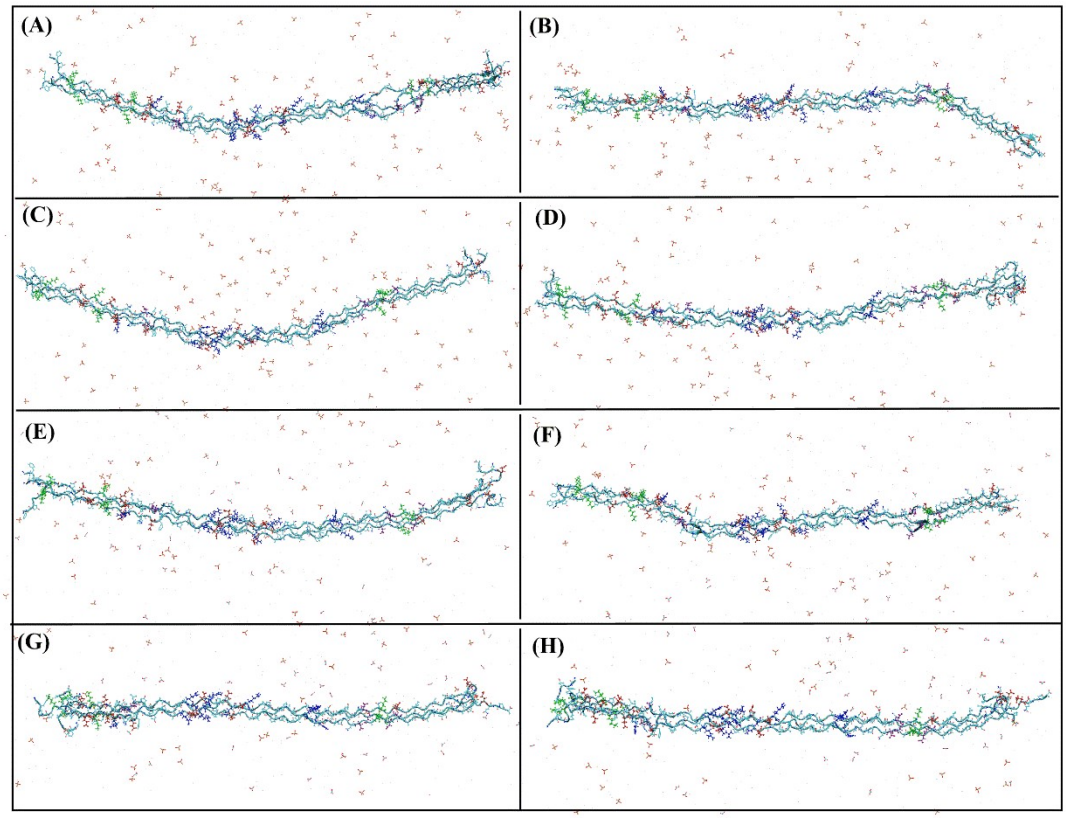

Figure S17. MD trajectory snapshots of other two replicas at 30 ns. (A) and (B) for model 1. (C) and (D) for model 2. (E) and (F) for model 3. (G) and (H) for model 4. For clarification, the Arg is coloured by blue, green for Lys, purple for Asp and red for Glu.

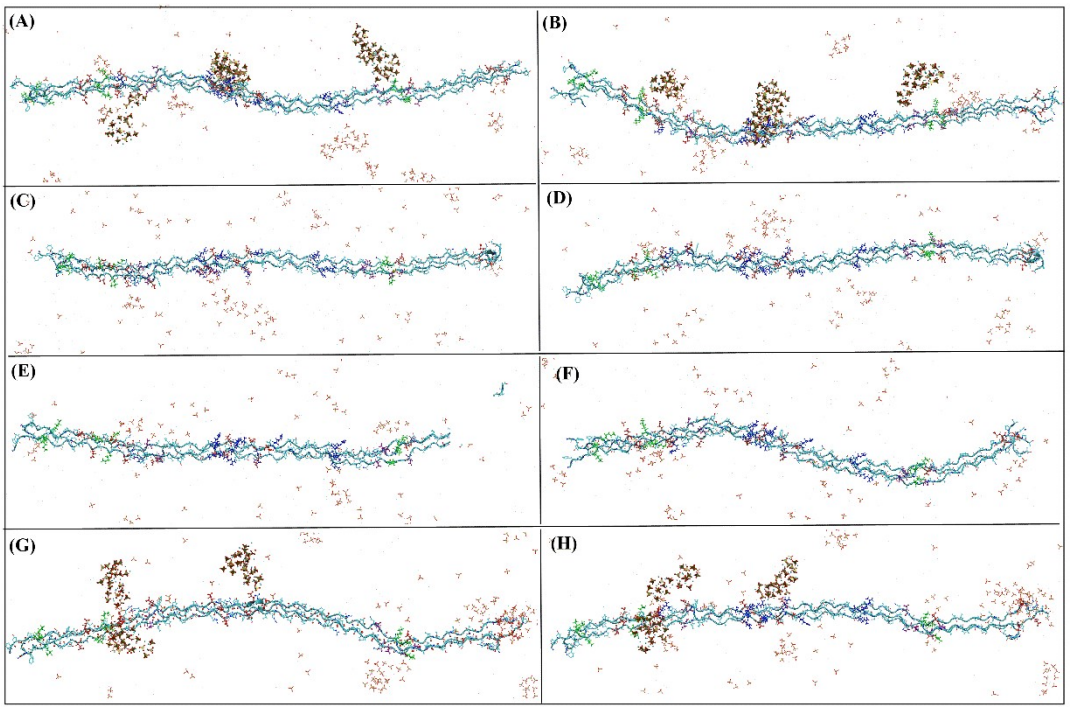

Figure S18. MD trajectory snapshots of other two replicas at 30 ns. (A) and (B) for model 5. (C) and (D) for model 6. (E) and (F) for model 7. (G) and (H) for model 8. For clarification, Arg is coloured blue, green for Lys, purple for Asp, and red for Glu.

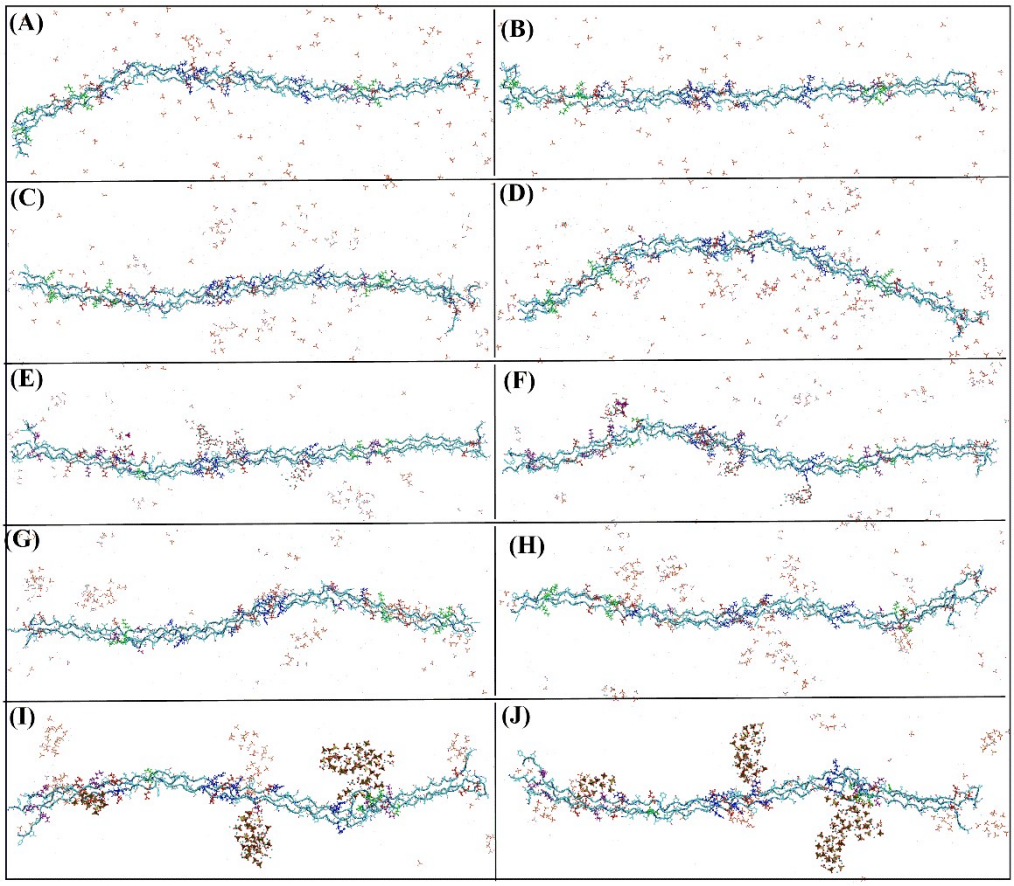

Figure S19. MD trajectory snapshots of other two replicas at 30 ns. (A) and (B) for model 9. (C) and (D) for model 10. (E) and (F) for model 11. (G) and (H) for model 12. (I) and (J) for model 13. For clarification, Arg is coloured blue, green for Lys, purple for Asp, and red for Glu.

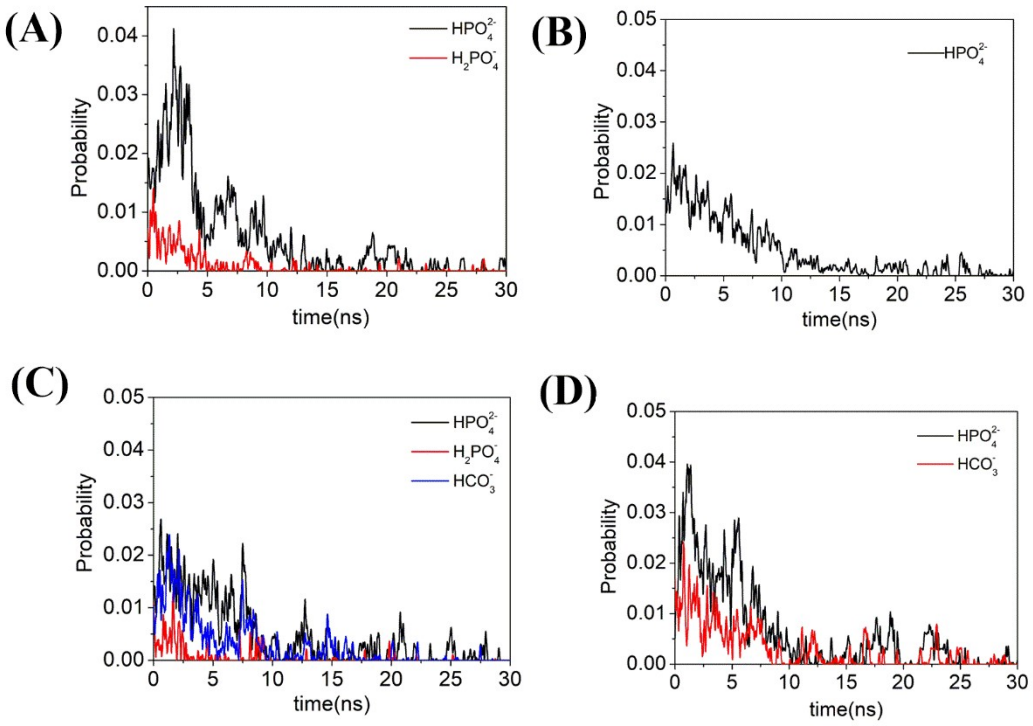

Figure S20. Evolution of the average values of the probabilities of various ions ($H_2PO_4^-$, HPO_4^{2-}, and HCO_3^-) in 30 ns molecular dynamics simulations of three replicas. (A) for Model 1, (B) for Model 2, (C) for Model 3, and (D) for Model 4.

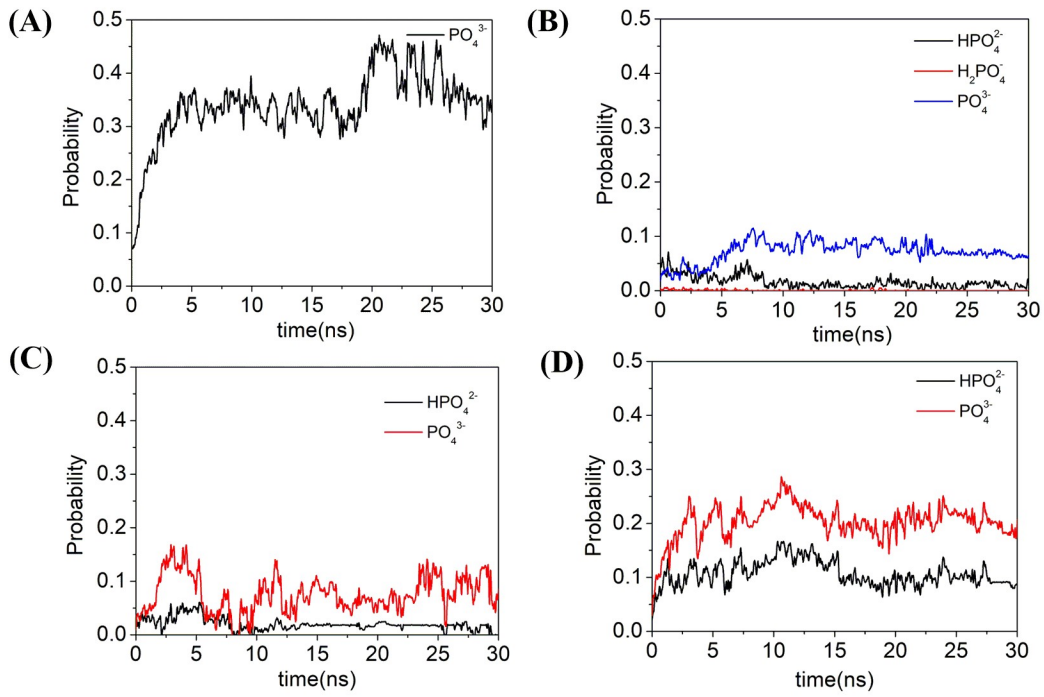

Figure S21. Evolution of the average values of the probabilities of various ions in 30 ns molecular dynamics simulations of three replicas. (A) Model 5, (B) Model 6, (C) Model 7, and (D) Model 8.

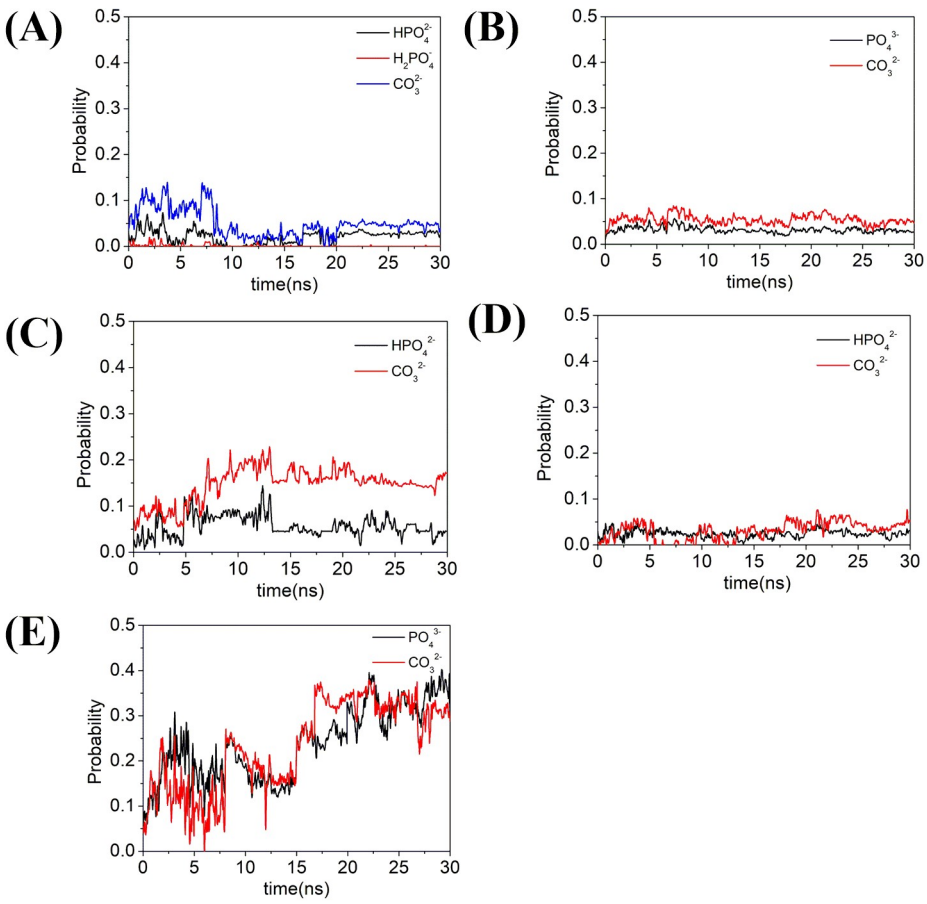

Figure S22. Evolution of average value of probability of various ions in 30 ns molecular dynamics simulations of three replicas (containing the initial model). (A) for Model 9, (B) for Model 10, (C) for Model 11, (D) for Model 12 and (E) for Model 13.

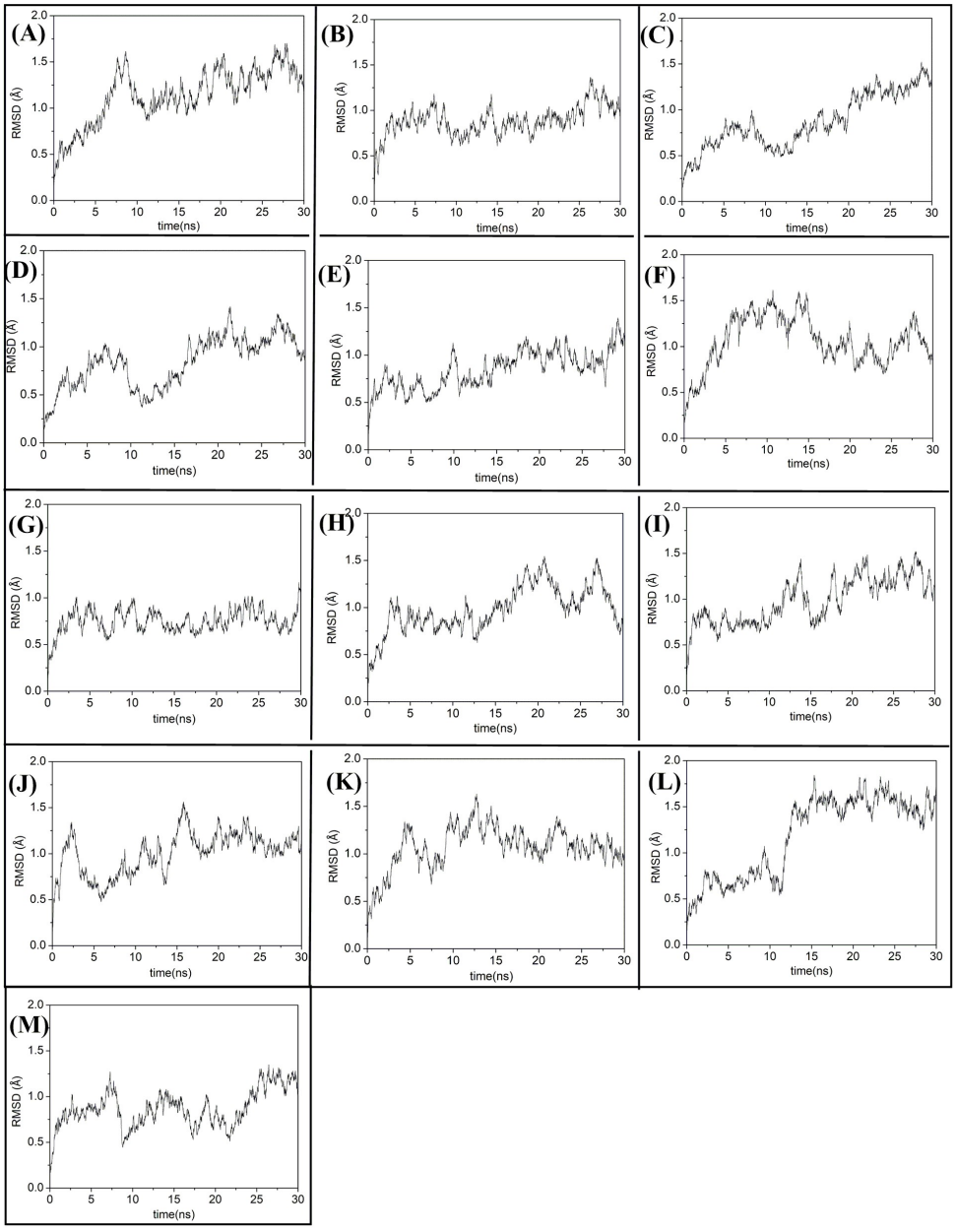

Figure S23. Root mean square deviations of backbone atoms of the 13 collagen models throughout 30 ns MD simulation. (A) Model 1, (B) Model 2, (C) Model 3, (D) Model 4, (E) Model 5, (F) Model 6, (G) Model 7, (H) Model 8, (I) Model 9, (J) Model 10, (K) Model 11, (L) Model 12, and (M) Model 13.

Table S1. The statistical average values for the probability evolution of each model at last 10 ns MD simulation

Models	Ions types	average value	standard deviation
Model 1	$H_2PO_4^-$	0.0	0.0
	HPO_4^{2-}	0.0	0.0
Model 2	HPO_4^{2-}	0.0	0.0
Model 3	$H_2PO_4^-$	0.0	0.0
	HPO_4^{2-}	0.0	0.0
Model 4	HCO_3^-	0.0	0.0
	HPO_4^{2-}	0.0	0.0
	HCO_3^-	0.0	0.0
Model 5	$H_2PO_4^-$	0.0	0.0
	HPO_4^{2-}	0.0841	0.0028
	PO_4^{3-}	0.0103	0.0088
Model 6	HPO_4^{2-}	0.0121	0.0075
	PO_4^{3-}	0.0715	0.0266
Model 7	HPO_4^{2-}	0.0624	0.0057
	PO_4^{3-}	0.133	0.0146
Model 8	PO_4^{3-}	0.535	0.0473
Model 9	$H_2PO_4^-$	0.0	0.0
	HPO_4^{2-}	0.0260	0.0058
	CO_3^{2-}	0.0451	0.0125
Model 10	HPO_4^{2-}	0.0240	0.0055
	CO_3^{2-}	0.0460	0.0108
Model 11	HPO_4^{2-}	0.0532	0.0080
	CO_3^{2-}	0.172	0.0052
Model 12	PO_4^{3-}	0.0288	0.0030
	CO_3^{2-}	0.0461	0.0063
Model 13	PO_4^{3-}	0.346	0.0376
	CO_3^{2-}	0.264	0.0547

Table S2. Definitions of models using combination of various anions in the

Labels	Model	Number							
		$n_{Ca^{2+}}$	$n_{H_2PO_4^-}$	$n_{HPO_4^{2-}}$	$n_{PO_4^{3-}}$	$n_{HCO_3^-}$	$n_{CO_3^{2-}}$	n_{Na^+}	
System 1	CMP-R/$H_2PO_4^-$	-	1	-	-	-	-	-	-
System 2	CMP-R/HPO_4^{2-}	-	-	1	-	-	-	1	-
System 3	CMP-R/PO_4^{3-}	-	-	-	1	-	-	2	-
System 4	CMP-R/CO_3^{2-}	-	-	-	-	-	1	1	-
System 5	CMP-R/HCO_3^-	-	-	-	-	1	-	1	1
System 6	CMP-R/$H_2PO_4^-$/ HPO_4^{2-}		1	1				2	
System 7	CMP-R /$H_2PO_4^-$/ HCO_3^-		1			1		1	
System 8	CMP-R / HPO_4^{2-}/ HCO_3^-			1		1		2	
System 9	CMP-R/$H_2PO_4^-$/PO_4^{3-}	-	1	-	1	-	-	3	-
System 10	CMP-R /HPO_4^{2-}/PO_4^{3-}	-	-	1	1	-	-	4	-
System 11	CMP-R /CO_3^{2-}/PO_4^{3-}	-	-	-	1	-	1	4	-
System 12	CMP-R/$H_2PO_4^-$/CO_3^{2-}		1				1	2	
System 13	CMP-R/HPO_4^{2-}/CO_3^{2-}			1			1	3	
System 14	Ca^{2+}/$H_2PO_4^-$	1	1	-	-	-	-	-	1
System 15	Ca^{2+}/HPO_4^{2-}	1	-	1	-	-	-	-	-
System 16	Ca^{2+}/PO_4^{3-}	1	-	-	1	-	-	1	-
System 17	Ca^{2+}/CO_3^{2-}	1	-	-	-	-	1	-	-
System 18	Ca^{2+}/HCO_3^-	1	-	-	-	1	-	-	1
System 19	Ca^{2+}/$H_2PO_4^-$/ HPO_4^{2-}	1	1	1				1	
System 20	Ca^{2+}/$H_2PO_4^-$/ HCO_3^-	1	1			1			
System 21	Ca^{2+}/ HPO_4^{2-}/ HCO_3^-	1		1		1		1	
System 22	Ca^{2+}/$H_2PO_4^-$/PO_4^{3-}	1	1	-	1	-	-	2	-
System 23	Ca^{2+}/HPO_4^{2-}/PO_4^{3-}	1	-	1	1	-	-	3	-
System 24	Ca^{2+}/CO_3^{2-}/PO_4^{3-}	1	-	-	1	-	1	3	-
System 25	Ca^{2+}/$H_2PO_4^-$/CO_3^{2-}	1	1				1	1	
System 26	Ca^{2+}/HPO_4^{2-}/CO_3^{2-}	1		1			1	2	

metadynamic